

Residual Correction in Real-Time Traffic Forecasting

Daejin Kim*
kiddj@kaist.ac.kr
KAIST AI
Republic of Korea

Youngin Cho*
choyi0521@kaist.ac.kr
KAIST AI
Republic of Korea

Dongmin Kim
tommy.dm.kim@kaist.ac.kr
KAIST AI
Republic of Korea

Cheonbok Park
cbok.park@navercorp.com
NAVER Corp.
Republic of Korea

Jaegul Choo
jchoo@kaist.ac.kr
KAIST AI
Republic of Korea

ABSTRACT

Predicting traffic conditions is tremendously challenging since every road is highly dependent on each other, both spatially and temporally. Recently, to capture this spatial and temporal dependency, specially designed architectures such as graph convolutional networks and temporal convolutional networks have been introduced. While there has been remarkable progress in traffic forecasting, we found that deep-learning-based traffic forecasting models still fail in certain patterns, mainly in event situations (e.g., rapid speed drops). Although it is commonly accepted that these failures are due to unpredictable noise, we found that these failures can be corrected by considering previous failures. Specifically, we observe autocorrelated errors in these failures, which indicates that some predictable information remains. In this study, to capture the correlation of errors, we introduce ResCAL, a residual estimation module for traffic forecasting, as a widely applicable add-on module to existing traffic forecasting models. Our ResCAL calibrates the prediction of the existing models in real time by estimating future errors using previous errors and graph signals. Extensive experiments on METR-LA and PEMS-BAY demonstrate that our ResCAL can correctly capture the correlation of errors and correct the failures of various traffic forecasting models in event situations.

CCS CONCEPTS

• Computer systems organization → Real-time system architecture; • Computing methodologies → Neural networks; Supervised learning by regression; • Mathematics of computing → Time series analysis; • Information systems → Sensor networks.

KEYWORDS

Traffic forecasting, Spatial-temporal forecasting, Graph neural networks, Residual autocorrelation

*Both authors contributed equally to this research.

Permission to make digital or hard copies of all or part of this work for personal or classroom use is granted without fee provided that copies are not made or distributed for profit or commercial advantage and that copies bear this notice and the full citation on the first page. Copyrights for components of this work owned by others than ACM must be honored. Abstracting with credit is permitted. To copy otherwise, or republish, to post on servers or to redistribute to lists, requires prior specific permission and/or a fee. Request permissions from permissions@acm.org.

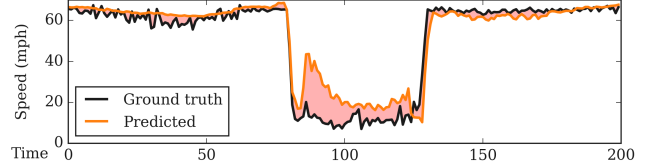
CIKM '22, October 17–21, 2022, Atlanta, GA, USA

© 2022 Association for Computing Machinery.

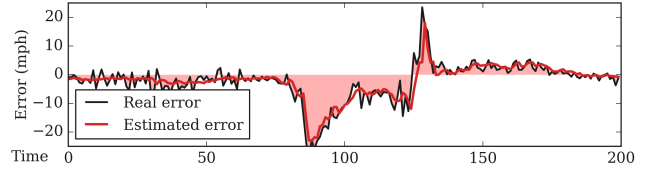
ACM ISBN 978-1-4503-9236-5/22/10...\$15.00

<https://doi.org/10.1145/3511808.3557432>

1. Traffic forecasting model (e.g., STGCN) makes erroneous predictions.



2-1. ResCAL: Estimate errors (real - prediction) from previous errors.



2-2. ResCAL: Calibrate the current predictions.

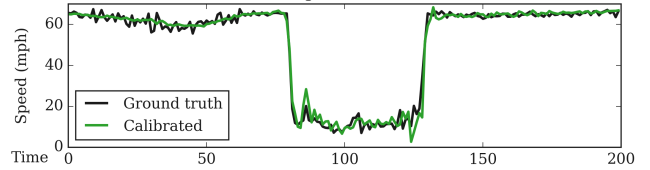


Figure 1: Using the pretrained traffic forecasting model, our proposed ResCAL calibrates the predictions by estimating the errors (residuals), i.e., failures of a model, and further improves the prediction performance. In traffic forecasting, predicting future errors is quite feasible since the previous errors from the model can be correlated with the current prediction.

ACM Reference Format:

Daejin Kim, Youngin Cho, Dongmin Kim, Cheonbok Park, and Jaegul Choo. 2022. Residual Correction in Real-Time Traffic Forecasting. In *Proceedings of the 31st ACM International Conference on Information and Knowledge Management (CIKM '22)*, October 17–21, 2022, Atlanta, GA, USA. ACM, New York, NY, USA, 10 pages. <https://doi.org/10.1145/3511808.3557432>

1 INTRODUCTION

Despite its high practicality, traffic forecasting is a complex task since the speeds of all nodes are highly dominated by their historical signals as well as the conditions of the neighboring nodes. To handle spatial-temporal datasets, recent studies [17, 18, 21, 26, 27, 30] introduce deep-learning-based models in traffic forecasting and consider the graph structure in the training process. While these studies have made great progress in the traffic forecasting task,

little attention has been given to analyzing the errors in the traffic forecasting models.

In this work, we analyze the errors in the traffic forecasting models and observe that recent models still produce relatively large errors in certain patterns regardless of their high average performance. While these failures are considered unpredictable, we found that we can estimate *how models will fail* using current errors. In the real world, it is presumable that correlations among successive errors (*i.e.*, failures) exist. However, previous errors have been ignored in the existing deep-learning-based traffic forecasting methods. Based on our findings, we highlight the necessity of utilizing previous errors in traffic forecasting. To explicitly handle the correlation of errors, we utilize historical errors of predictions, *i.e.*, residuals, to make the next prediction. This can correct the failures of the traffic forecasting models and improve their performance in unexpected situations. Consequently, the critical mistakes that are crucial in a real-time setting can be minimized.

In addition to the previous predictions within a single sensor node, the previous predictions of the neighboring nodes are also highly correlated with the current prediction of each sensor node. To consider both spatial and temporal residual correlations, we propose a simple residual estimation module called ResCAL that estimates the expected residuals in the current prediction, *i.e.*, how forecasting models will fail. Our method adopts the spatial-temporal layers conducted with a gated temporal convolutional network (Gated TCN) and a graph convolutional layer (GCN), as proposed in [26]. Furthermore, we analyze the patterns of failures since high errors occur in certain patterns. To this end, we introduce vector quantization in ResCAL and provide the justification of the calibrations. Vector quantization also allows our method to handle the noise and the outliers that appear in residuals.

Fig. 1 depicts how ResCAL corrects the failures in the real-time setting. Several attempts have been made to consider the residuals in graph classification [9, 13]; however, to the best of our knowledge, this study is the first attempt to capture the temporal correlation of residuals in traffic forecasting. In our experiments, we confirm that the residuals of each node are highly correlated with its previous residuals as well as that of neighboring nodes. Here, we introduce a simple synthetic dataset and validate the correctness of our ResCAL both qualitatively and quantitatively. Subsequently, we conducted extensive experiments in the two most representative traffic datasets: METR-LA and PEMS-BAY. In both datasets, we calibrated the predictions from various traffic forecasting models such as STGCN [27], DCRNN [17], Graph WaveNet [26], and STAWnet [21]. Specifically, we focus on whether our ResCAL accurately calibrates the predictions in the time areas where the existing models struggle. Despite its simplicity, our ResCAL consistently improves performance in event situations. Along with correcting failures, we validate the effectiveness of the vector quantization approach with a qualitative analysis. In this analysis, we verify that our ResCAL can provide meaningful justification for the calibration by examining the residual patterns in the unobserved data.

Our contributions can be summarized as follows:

- We highlight the importance of utilizing the historical predictions to explicitly handle the correlation among errors that occur in a real-time setting.
- We propose a novel method called ResCAL as a widely-applicable add-on module, which estimates the future residuals and corrects the failures of models.
- Extensive experiments demonstrate that our ResCAL consistently improves the baselines in event situations while significantly reducing the correlation of residuals.

2 RELATED WORKS

2.1 Traffic Forecasting

Traffic forecasting is a challenging task due to the complicated spatial and temporal dependencies among the sensor nodes. To capture the dynamics of traffic conditions, data-driven approaches based on deep learning have received considerable attention. In spatial and temporal modeling, approaches based on graph convolutional networks (GCNs) [1, 16, 28] are promising in capturing spatial dependencies among roads. Several studies [5, 25, 29] have proposed applying recurrent neural networks (RNNs) and convolutional neural networks (CNNs) to capture the temporal dependencies along the sequence in traffic forecasting.

Recent studies [17, 18, 21, 26, 27, 30] have shown that graph modeling is a key factor to achieve state-of-the-art performance in traffic forecasting. Particularly, DCRNN [17] demonstrates its impressive performance against statistical approaches by incorporating diffusion graph convolutional neural networks [1] into RNNs. STGCN [27] utilizes only convolution-based approaches for modeling spatial and temporal dependencies in the road network. Graph WaveNet [26] introduces a self-adaptive adjacency matrix to overcome the limitation of applying fixed adjacency information and uses dilated convolutions [22] to efficiently handle long sequences. As another approach, STAWnet [21] applies a self-attention mechanism [24] to capture spatial dependencies between roads and uses self-learned node embedding to eliminate the need of prior knowledge of the graph structure. While these studies have shown remarkable progress in solving the traffic forecasting problem, methods to consider the errors of the forecasting models have been under-explored. In the line of traffic forecasting research, our work can improve the performance of the existing forecasting models by calibrating predictions of those models in real time.

2.2 Residual Correction

In statistical approaches, residual is defined as the difference between the ground truth values and the predicted ones. Statistical time-series models such as the autoregressive model and moving-average model represent future values as a linear combination of observed values and residuals at previous times steps. The autoregressive integrated moving average (ARIMA) [2] model considers residuals with autoregressive terms. However, these approaches suffer from expressing non-linearity because the residual term is expressed as a finite linear combination of a white-noise sequence.

Fitting residuals in the regression problem is an effective technique in machine learning. For example, a gradient boosting algorithm [6] and its variants, such as XGBoost [3] and LightGBM [14], recursively capture the residuals to improve the performance. Moreover, graph neural network architectures to model residual correlation have also been proposed. [13] suggested modeling of the joint distribution of the residuals to obtain information from both the

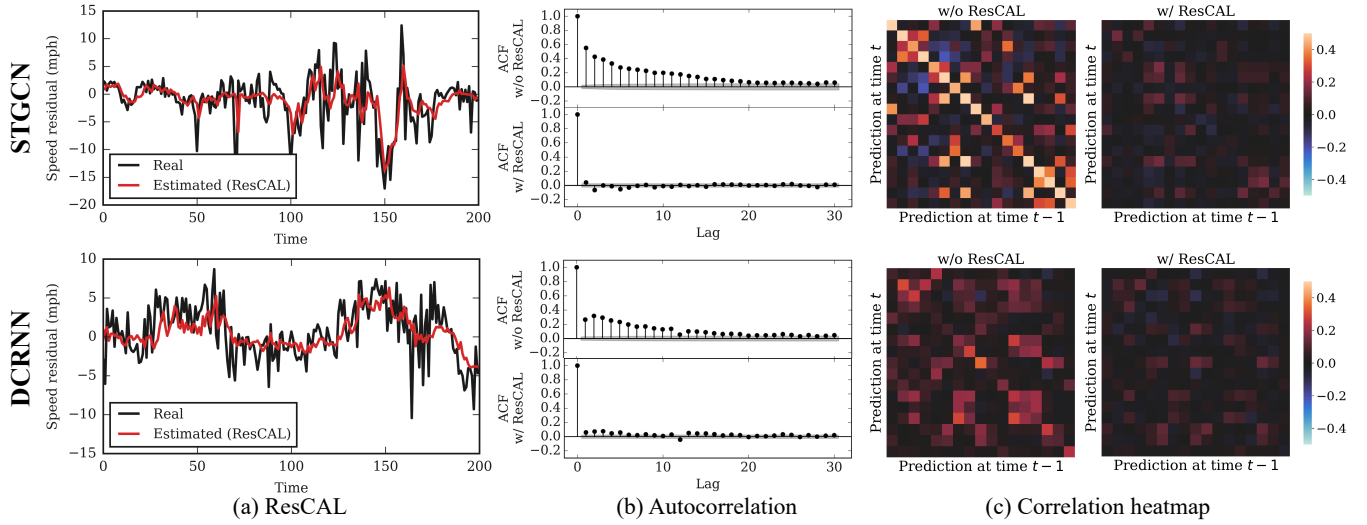


Figure 2: Reduction in the autocorrelation of residuals on the METR-LA dataset. We analyzed the 5 minutes ahead prediction results on node 19, and node 22 for STGCN, and DCRNN, respectively. (a) plots the ground truth residual and the estimated residual for each case, and shows that our proposed ResCAL accurately estimates the residual for both cases. (b) represents the ACF plots of residuals with and without the calibration of ResCAL. After applying ResCAL, the autocorrelation at every lag decreases to almost zero, indicating temporal dependencies are captured by ResCAL. (c) shows the heatmaps of lag 1 autocorrelation of residuals on a neighborhood of node 19 for STGCN, and node 22 for DCRNN. (i, j) -th element of the heatmap shows a Pearson Correlation of residuals between the i -th node at time t and j -th node at time $t - 1$. The brighter point represents a high correlation between the two corresponding nodes. For both cases, ResCAL drastically reduces the correlation between these nodes, indicating that ResCAL can capture both temporal and spatial dependencies to correct the predictions.

input feature and the output correlation in the graph structure. [9] proposes a procedure called “Correct and Smooth”, which models error correlation to correct the base prediction from simple architectures such as multi-layer perceptron (MLP). In contrast to these works, our ResCAL considers both spatial and temporal residuals to enhance the performance of traffic forecasting models.

2.3 Discrete Representations

Utilizing the discrete representation can provide interpretability and reduce the noise for a given data [4, 12, 23]. One of the discretization approaches is vector quantization [7], which is suggested as a system for mapping a signal into a digital sequence. VQ-VAE [23] utilizes this quantization mechanism to model the categorical distribution, and the latent variable is represented as the combination of the embedding vectors. The vector quantization layer formulates a latent space, called codebook, and clusters vectors according to a given distance metric (e.g., L2 distance). To learn a discrete representation by the backpropagation algorithm, [12] suggests Gumbel-Softmax which can approximate categorical samples by a differentiable sampling mechanism. In this work, we utilize discrete representation to enhance the interpretability of the calibration module and to reduce the noise introduced in traffic forecasting.

3 RESIDUAL DIAGNOSTICS IN TRAFFIC FORECASTING

High Errors in Traffic Forecasting. In the real world, a few critical errors have a huge influence on traffic conditions. Therefore,

predicting such errors is essential for the traffic forecasting task. On a widely used traffic dataset, METR-LA [17], we observed that top-20% errors account for about 60% of the total absolute errors, e.g., 63.0% for STGCN and 62.8% for DCRNN. In traffic dynamics, these abnormal cases are mainly caused by sparse events. In this work, we specifically focus on time steps with top-20% errors and denote them as *event situations* since a large magnitude of error indicates the failure of the prediction.

Residual Autocorrelation in Traffic Forecasting. Autocorrelation is the correlation of a time series and its delayed copy. Given an input sequence y_1, y_2, \dots, y_T , the autocorrelation function (ACF) r_k measures the degree of the linear relationship between y_t and y_{t-k} where k is a time lag:

$$r_k = \frac{\sum_{t=k+1}^T (y_t - \bar{y})(y_{t-k} - \bar{y})}{\sum_{t=1}^T (y_t - \bar{y})^2}. \quad (1)$$

High autocorrelation indicates a high potential of performance improvement; any forecasting model of which residuals are correlated or residuals have a non-zero mean can be improved by estimating the future residuals [10]. The residuals of the traffic forecasting model are commonly autocorrelated; therefore, we explicitly capture this relationship to further enhance the model performance.

Fig. 2 (b) shows the ACF of residuals for the traffic forecasting models. Before calibration, the residuals have a high autocorrelation, meaning that predictable information remains in the residuals. Fig. 2 (c) represents the Pearson Correlation between the current residual of each sensor node and the previous residuals of neighboring sensor nodes on METR-LA. The bright points in the heatmap

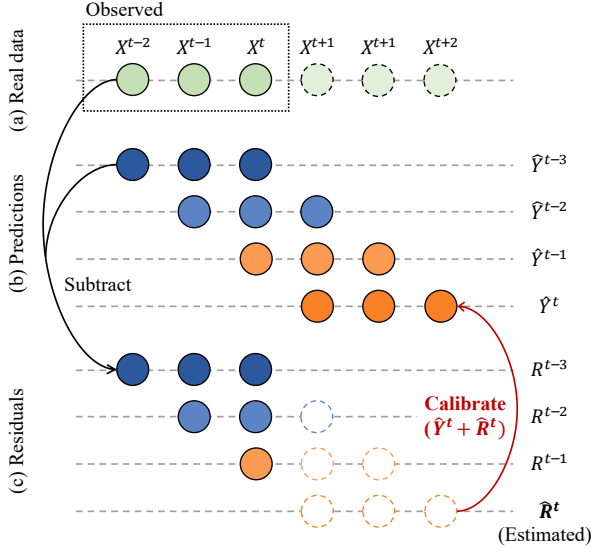


Figure 3: Estimation of residuals at time t . Residuals (c) available at time t are based on previous predictions (b) and observed real data (a). The aim of ResCAL is to make an estimation on the residuals for the current prediction.

of the existing forecasting models show that the residuals in the neighboring sensor nodes are highly correlated. By calibrating the predictions, the correlation among the residuals can be significantly reduced, as shown in the ACF plot and the heatmap.

4 RESIDUAL CORRECTION IN TRAFFIC FORECASTING

In this section, we introduce a simple model-agnostic framework to boost the performance of traffic forecasting models in the real-time setting. To this end, we first formally describe the problem setting considered in traffic forecasting. Next, the model architecture and the residual prediction mechanism of our ResCAL are introduced.

4.1 Real-Time Traffic Forecasting

The aim of traffic forecasting is to predict the future traffic speed observed at N correlated sensors on the road network. Let $\mathcal{G} = (\mathcal{V}, \mathcal{E})$ be a graph representing the spatial relationship between sensors where \mathcal{V} is a set of nodes ($|\mathcal{V}| = N$) and \mathcal{E} is a set of edges. Following the convention of the traffic prediction problem, $X^t \in \mathbb{R}^{N \times 2}$ is denoted as the graph signal obtained at time t ; $X_{:,1}^t$ and $X_{:,2}^t$ represent the speed and the timestamp features, respectively. The goal of traffic forecasting is to learn a mapping function f from past graph signals and a graph \mathcal{G} to future traffic speeds:

$$[X^{(t-T_x+1):t}, \mathcal{G}] \xrightarrow{f} X_{:,1}^{(t+1):(t+T_y)}, \quad (2)$$

where T_x and T_y are the input and output sequence lengths, respectively. In particular, we consider a real-time traffic forecasting problem in which the current prediction of the model can be corrected using continuous historical predictions. Let $Y^t = X_{:,1}^{(t+1):(t+T_y)} \in \mathbb{R}^{N \times T_y}$ be the ground truth speed so that $Y_{:,i}^t$ represents the ground

truth speed of i step ahead prediction at time t , and \hat{Y}^t is its estimated values, i.e., $\hat{Y}^t = f(X^{(t-T_x+1):t}, \mathcal{G})$. Then, the residual of traffic prediction is defined as $R^t = Y^t - \hat{Y}^t$. Note that the ground truth of $R_{:,i}^t$ can be observed when time is greater than or equal to $t + i$. $U^t = [R_{:,1}^{(t-1)}, R_{:,2}^{(t-2)}, \dots, R_{:,T_y}^{(t-T_y)}] \in \mathbb{R}^{N \times T_y}$ is denoted as the newly observed residuals at time t . Here, our main problem is learning a mapping function g which predicts the residual at time t , given past graph signals, observed residuals, and a graph \mathcal{G} :

$$[X^{(t-T_x+1):t}, U^{(t-T_u+1):t}, \mathcal{G}] \xrightarrow{g} R^t, \quad (3)$$

where T_u is the time steps of the observed residuals. Given the estimated residuals $\hat{R}^t = g(X^{(t-T_x+1):t}, U^{(t-T_u+1):t}, \mathcal{G})$, accurate predictions can be made by taking $\hat{Y}^t + \hat{R}^t$ as a final output. Fig. 3 illustrates our problem setting.

Our proposed problem setting in real-time traffic forecasting has several advantages, as follows: (i) The correlation between successive residuals can be explicitly modeled. We may consider resizing the window size of input to handle this correlation in the time series model. However, this can be tricky depending on the model design and is time-consuming to retrain due to its high complexity. (ii) As most parts of the complex modeling is done by f , we can learn g with a relatively lightweight model to estimate the residuals. This allows hyperparameter tuning with a small budget and increases the reusability of the model in real-world situations. (iii) Since information about f is not needed to predict the residuals, the performance of the base forecasting model can be improved in a model-agnostic way.

4.2 ResCAL

To explicitly model the residuals, we designed a light-version of the traffic forecasting model called ResCAL consisting of spatial-temporal layers with the self-adjacency matrix, as proposed by [26]. The overall architecture of our ResCAL is depicted in Fig. 4. The encoder consists of k spatial-temporal layers, each conducted by a gated temporal convolutional layer (Gated TCN) and a graph convolutional layer (GCN). Following the conventional setting of the base traffic forecasting models, we let $T = T_x = T_y$. The encoder produces a latent $Z \in \mathbb{R}^{N \times d_h}$ by taking both a graph signal $X \in \mathbb{R}^{N \times 2 \times T}$ and a residual $U \in \mathbb{R}^{N \times T_u \times T}$:

$$Z = \text{Encoder}(\text{Concat}(X, U)), \quad (4)$$

where **Concat** is a concatenation operation along the second axis and d_h is the number of hidden dimensions.

Here, we want to make a more accurate prediction by capturing useful information from Z and simultaneously provide a reason for the judgment. However, it is difficult to directly analyze Z since we do not put any strict restrictions on generating Z . Moreover, the noise introduced by the baseline model or data further hinders the analysis of Z . Previous works [12, 23] introduce discrete latent vectors into an autoencoder to increase the interpretability and stabilize training on the noisy data. However, we observe that using only these discrete forms sometimes reduces overall performance of the model. Instead, we use a hybrid approach of combining discrete and continuous representations. We take the sum of the outputs of two different branches from Z : the regression branch and the quantization branch. The regression branch provides a

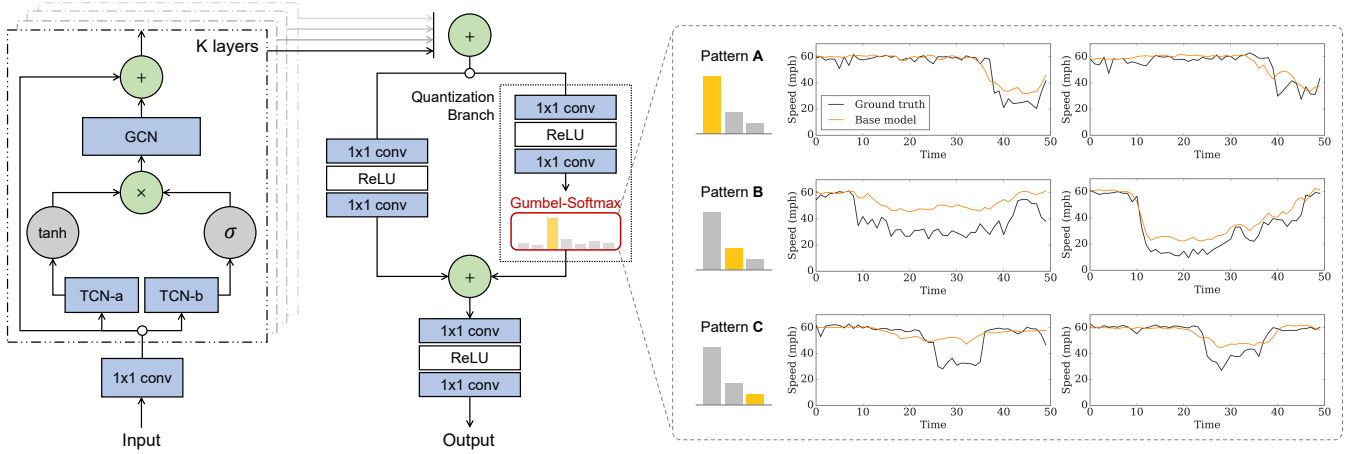


Figure 4: The overall architecture of our ResCAL. The encoder consists of spatial-temporal layers and the decoder with the quantization branch outputs the residuals expected to occur in the following predictions. The quantization branch with Gumbel-Softmax operation classifies the patterns of events and provides the interpretation of the events and the failures of the base models.

continuous representation of the accurate estimation of the residual while the quantization branch provides interpretable and denoised information using discrete representation. The Straight-Through (ST) Gumbel estimator [12] is used to provide the differentiable discrete variable $y \in \{0, 1\}^k$ given an input $x \in \mathbb{R}^k$:

$$y = \text{ST-Gumbel}(x) = \text{one_hot}(\text{argmax}_i [g_i + x_i]), \quad (5)$$

where g_1, g_2, \dots, g_k are i.i.d samples drawn from the standard Gumbel distribution. This variable is smoothly approximated in the backward pass. Formally, with the learnable embedding vector $E \in \mathbb{R}^{d_e \times (d_c \times n_c)}$, the quantized vector $Q \in \mathbb{R}^{N \times (d_c \times n_c)}$, the estimated future residual $R \in \mathbb{R}^{N \times T_y}$, and the output of ResCAL is calculated as:

$$\begin{aligned} W &= f_q(Z), \\ R &= f_o(f_r(Z) + QE^T), \\ Q_{i,j_k+1:j_k+n_c} &= \text{ST-Gumbel}(W_{i,j_k+1:j_k+n_c}), \end{aligned} \quad (6)$$

where n_c is the number of categories, d_c is the number of categorical variables, d_e is the dimension of the embedding matrix, and $j_k := k \cdot n_c$ for $k = 0, \dots, d_c - 1$; f_o , f_r , and f_q are the output layer, regression layer, and quantization layer, respectively. Each layer consists of a combination of a pointwise convolution and a ReLU activation.

By predicting the residuals, we can easily calibrate the models and further improve the existing traffic forecasting models. In real-time prediction, the previous residuals emerged by the prediction model as well as the current traffic data are used as the input and the future residuals are predicted. The clustering results can also be used to interpret the behavior of the model. In Section 6, we will show that the baselines fail similarly for similar events. Using the predicted residuals, we can now calibrate the output of the prediction model. By calibrating the future prediction with the current errors, we can consider the temporal dependency between residuals in traffic forecasting. Our experiments show that such improvements cannot be achieved solely by increasing the capacity of the base forecasting model with additional parameters or utilizing

Table 1: Detailed description of the synthetic data, METR-LA and PEMS-BAY used in our experiments.

Data	# Nodes	# Edges	# Time steps
Synthetic	-	-	10000
METR-LA	207	1515	34272
PEMS-BAY	325	2369	52116



Figure 5: Sensor locations of (a) METR-LA and (b) PEMS-BAY.

longer sequences of the input without considering the temporal dependencies of the residuals as our ResCAL does.

5 EXPERIMENTAL SETTINGS

5.1 Traffic Dataset

We examined our ResCAL on the two representative traffic datasets: PEMS-BAY and METR-LA introduced by [17]. PEMS-BAY, collected by California Transportation Agencies (CalTrans) Performance Measurement System (PeMS), contains 325 sensor data from the Bay Area. In our experiments, 6 months of data collected from Jan 1st, 2017 to May 31st, 2017 was selected. METR-LA contains the traffic speed data recorded by 207 sensors on the highways of Los Angeles County [11]. The sensor locations of METR-LA and PEMS-BAY are shown in Fig. 5. Both datasets were preprocessed following [17]. For METR-LA, 4 months of data collected from Mar 1st, 2012 to Jun 30th, 2012 was selected for our experiments. For both datasets, the traffic speed is aggregated into 5 minute windows, and Z-score normalization is applied to the input. As [19] proposed, adjacency matrix of both datasets was conducted using road distances with a threshold Gaussian kernel. A detailed description of each dataset is provided in Table 1.

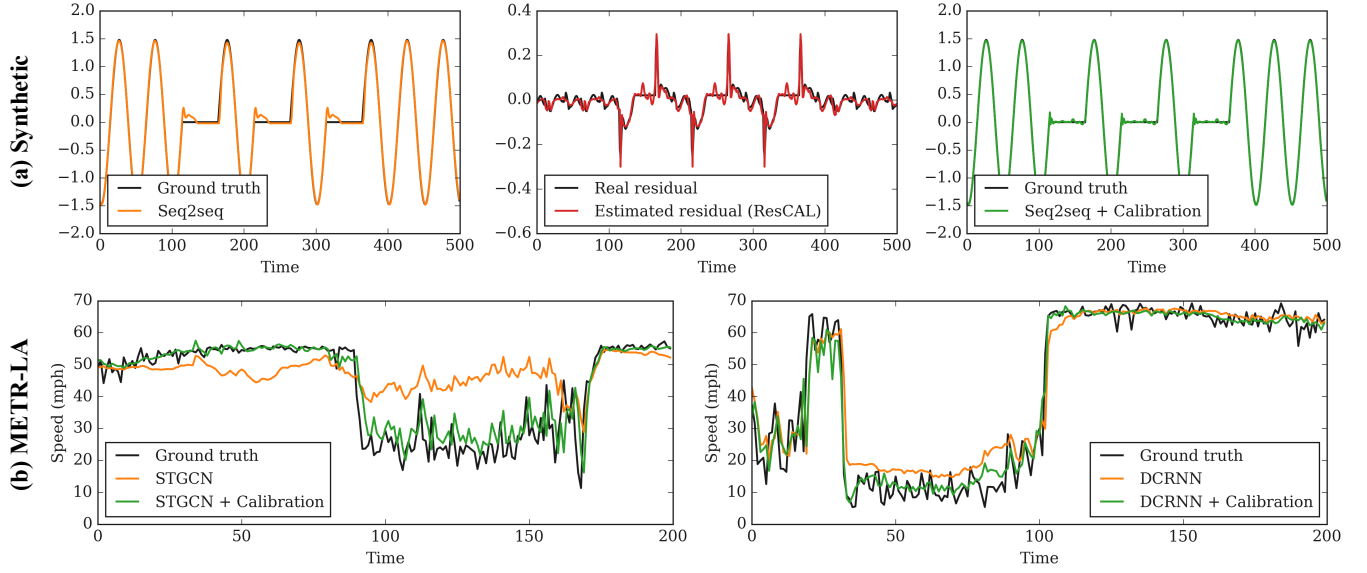


Figure 6: Calibrated predictions using ResCAL. (a) On the synthetic dataset, Seq2Seq shows similar failures for each event, and ResCAL correctly calibrates the predictions. (b) On METR-LA, ResCAL accurately corrects the failures of the baseline models.

5.2 Baseline Methods

To widely validate the correctness and effectiveness of our ResCAL, we examined several baselines commonly used for traffic forecasting. We additionally provide the reported results for the basic models such as ARIMA and FC-LSTM to help compare the performance of various models. In this work, we choose the mean squared error (MSE) for training the base models. For all baselines, the PyTorch implementation was utilized as denoted in their footnotes, and their default training strategies were followed.

- **ARIMA**. The auto-regressive integrated moving average model with a Kalman filter, which is the most representative regression model for time series data.
- **FC-LSTM [20]**. Basic deep-learning-based regression model for time series data conducted with long short-term memory (LSTM) [8] and fully-connected layers.
- **DCRNN [17]**.¹ Diffusion convolutional recurrent neural network consisting of the graph convolutional networks and recurrent neural networks.
- **STGCN [27]**.² Spatial-temporal graph convolutional network which is conducted with the graph convolutional layer and 1D convolutional layers.
- **Graph WaveNet [26]**.³ Traffic forecasting model which combines the dilated 1D convolutional layers and graph convolutional networks.
- **STAWnet [21]**.⁴ Spatial-temporal attention network with temporal convolution and spatial attention mechanism to capture dynamic spatial dependencies.

¹github.com/chnsh/DCRNN_PyTorch

²github.com/FelixOpolka/STGCN-PyTorch

³github.com/nanzhan/Graph-WaveNet

⁴github.com/CYBruce/STAWnet

Table 2: Experimental results on the synthetic dataset for LSTM Seq2seq with and without our ResCAL.

Time steps	Models	MAE	RMSE	MAPE
1 step	Seq2seq	0.029	0.047	7.37%
	+ Calibration	0.015	0.022	2.95%
6 step	Seq2seq	0.061	0.153	20.34%
	+ Calibration	0.025	0.093	10.29%
12 step	Seq2seq	0.123	0.294	51.70%
	+ Calibration	0.067	0.205	27.56%
24 step	Seq2seq	0.174	0.367	80.64%
	+ Calibration	0.122	0.291	53.47%

5.3 Training Settings

For both METR-LA and PEMS-BAY, we used the same training strategy for the simplicity. $k = 4$ spatial-temporal layers were used for the encoder, and $d_c = 32$, $n_c = 16$, and $d_e = 16$ were set for the quantization branch in the decoder. Since the baselines predict the next $T = 12$ steps in units of 5 minutes and each step has errors of 12 horizons, the input residuals and predictions have a size of 12×12 and 12×1 , respectively. Our ResCAL is trained with the mean absolute error (MAE) and a batch size of 256. An Adam optimizer with a learning rate of 0.001, $\beta_1 = 0.9$ and $\beta_2 = 0.999$ is also used. Each dataset is split into a training set, validation set, and test set with a ratio of 7:1:2 and the model with the best validation score is selected in all experimental evaluations.

6 EXPERIMENTAL RESULTS

6.1 Synthetic Dataset

To validate the correctness of our ResCAL, we first construct a simple synthetic dataset where similar events are occurring at random

Table 3: Quantitative results in event situations where the absolute error of the base forecasting model falls within the top 20%. The performances of the forecasting models were measured with and without our ResCAL on the METR-LA and PEMS-BAY datasets. The results are reproduced as mentioned in Section 5. Note that the high error region depends on the base forecasting model.

Data	Models	15min			30min			60min			Average		
		MAE	RMSE	MAPE	MAE	RMSE	MAPE	MAE	RMSE	MAPE	MAE	RMSE	MAPE
METR-LA	DCRNN [17]	14.53	16.31	48.63%	16.98	18.93	60.79%	20.03	22.00	75.27%	17.18	19.08	61.56%
	+ Calibration	13.46	15.44	44.22%	16.26	18.38	57.37%	19.45	21.54	73.13%	16.39	18.46	58.24%
	STGCN [27]	15.29	16.93	53.19%	17.94	19.78	65.91%	21.17	23.00	82.76%	18.13	19.90	67.29%
	+ Calibration	12.77	15.07	43.55%	15.79	18.18	57.50%	19.10	21.44	73.93%	15.88	18.23	58.33%
	Graph WaveNet [26]	13.39	15.06	41.49%	16.15	17.99	54.92%	19.08	20.93	69.24%	16.21	17.99	55.22%
	+ Calibration	13.28	14.99	41.45%	16.03	17.93	54.43%	18.94	20.85	68.34%	16.08	17.93	54.74%
	STAWnet [21]	13.56	15.30	43.75%	16.15	18.10	56.00%	19.00	21.00	68.44%	16.24	18.13	56.06%
	+ Calibration	13.17	14.98	42.24%	15.87	17.89	54.88%	18.80	20.84	68.21%	15.95	17.90	55.11%
	DCRNN [17]	4.41	6.07	10.51%	5.95	8.45	15.36%	7.50	10.53	20.39%	5.95	8.35	15.42%
	+ Calibration	4.25	5.93	10.07%	5.65	8.15	14.37%	6.94	10.00	18.60%	5.61	8.03	14.34%
PEMS-BAY	STGCN [27]	6.42	7.95	15.88%	7.50	9.44	19.39%	8.74	11.03	23.50%	7.56	9.47	19.59%
	+ Calibration	3.88	5.91	9.55%	5.41	8.00	14.36%	6.84	9.78	18.94%	5.38	7.90	14.29%
	Graph WaveNet [26]	4.36	5.89	10.45%	5.72	7.97	14.46%	6.89	9.50	18.07%	5.66	7.79	14.33%
	+ Calibration	4.28	5.87	10.07%	5.63	7.93	14.21%	6.81	9.46	18.02%	5.57	7.75	14.10%
	STAWnet [21]	4.38	5.96	10.34%	5.71	7.91	14.51%	6.75	9.29	18.07%	5.61	7.72	14.31%
	+ Calibration	4.27	5.87	10.07%	5.62	7.88	14.23%	6.70	9.27	17.77%	5.53	7.67	14.02%

time steps. This reflects the nature of traffic data which has a similar propagation of congestion in cases of accidents.

Concretely, the synthetic dataset with the lengths of 10k time steps contains a periodic sine wave with a randomly generated zero signal, as depicted in Fig. 6 (a). The period of the sine wave is set to 50 steps and each period with zero values is randomly substituted with a probability of 0.1 to reflect the traffic dynamics. Similar to the traffic datasets, the synthetic dataset is divided into three parts: the training set, validation set, and test set with a ratio of 7:1:2. With our synthetic dataset, we examine the correctness of the following two assumptions essential for residual correction: (i) a deep-learning-based prediction model likely generates similar errors in similar types of events, and (ii) when the residuals are correlated, it is possible to improve the performance of the base prediction model by estimating the residuals that will occur, *i.e.*, *how the model fails*.

For the base prediction model, we build a simple sequence-to-sequence model (Seq2seq). Seq2seq is designed to get an input sequence of length 24 and generate predictions on the next 24 steps. The encoder and decoder of Seq2seq are conducted with GRU units with a hidden feature size of 128 and a single recurrent layer. The output of the decoder is passed to a multi-layer perceptron (MLP) consisting of ReLU activations and fully connected layers of size 128-16-1. The model is trained using an Adam optimizer [15] with a learning rate of 0.001, $\beta_1 = 0.9$, $\beta_2 = 0.999$, and a batch size of 100. The model is trained for 50 epochs and the Z-score normalization is applied to preprocess the input.

Fig. 6 (a) shows the predictions of the Seq2seq model, the estimated residuals from our ResCAL, and the calibrated prediction,

respectively. As we expected in the first assumption, the prediction model always made similar errors for similar types of events. This implies that the residuals do not occur randomly and are also predictable. To assess the second assumption, we trained our ResCAL to predict the residuals occurring in Seq2seq. For the synthetic dataset without the graph structure, the spatial-temporal layers in the encoder were replaced with 1D convolutional layers. We set $d_c = 32$, $n_c = 16$, and $d_e = 16$ for the quantization branch in the decoder. For training, an Adam optimizer with a learning rate of 0.001 and a batch size of 128 was used. Since the length of Seq2seq is $T = 24$ steps, our ResCAL gets 24×24 residuals with the original time series data for the input and outputs the 24×1 size of the residuals. Table 2 shows the results of Seq2seq with and without our ResCAL. Our ResCAL is shown to greatly enhance the performance of Seq2seq in every step of the predictions. This indicates that our ResCAL accurately predicts the residuals to occur. Notably, our ResCAL further improves the MAE of Seq2seq by 0.014, 0.036, 0.056, and 0.052 for 1 step, 6 steps, 12 steps, and 24 steps, respectively. Through a simple simulation, we validate that our assumptions and the proposed method are quite presumable in the time series data. The calibrated results in Fig. 6 (a) demonstrate that repeated errors can be estimated by our ResCAL. Moreover, the experiments on the synthetic data show that ResCAL allows the model to rapidly adapt to unexpected changes.

6.2 Traffic Dataset

In this section, we demonstrate that our ResCAL can correct the failure of the existing traffic forecasting models on the METR-LA

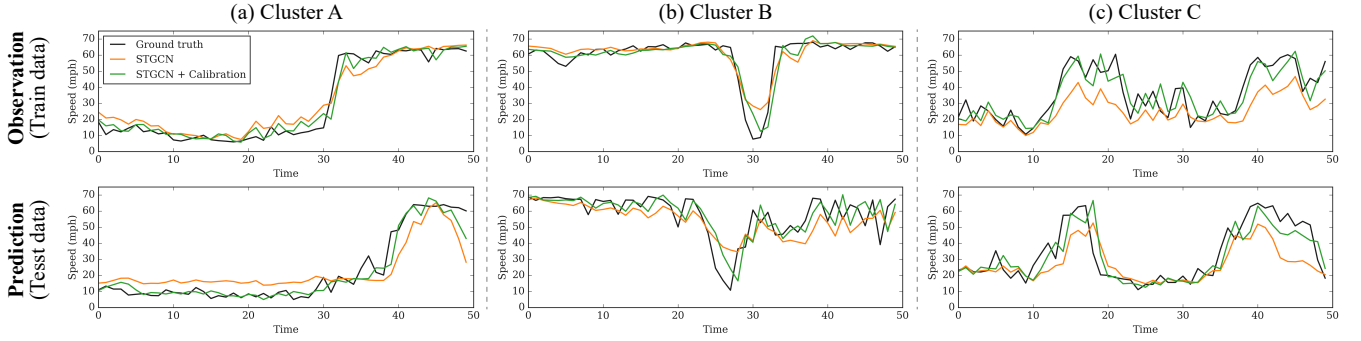


Figure 7: The calibration results on the train dataset and test dataset of the METR-LA dataset. Each pair in (a), (b), and (c) contains two different results assigned in the same pattern. Events of the same pattern in the train dataset can be interpreted as *evidences* of the calibration of our ResCAL in real-time traffic forecasting.

and PEMS-BAY datasets. Our ResCAL is trained with the settings as described in Section 5.

Residual Correction in Event Situations. To reflect the nature of the real-world setting, we examine our ResCAL in regions where critical errors occur. Table 3 shows the calibration results on time steps where the absolute error of the base forecasting model falls within the top 20%. Surprisingly, we can observe large gaps in performance before and after calibration. In the event situations on METR-LA, our ResCAL improves the performance of DCRNN by 0.79, 0.62 and 3.32% for MAE, RMSE, and MAPE, respectively. Even for STAWnet, the most advanced traffic forecasting model, our ResCAL shows an improvement of 0.29, 0.23 and 0.95% for MAE, RMSE, and MAPE on METR-LA, respectively. Consequently, our ResCAL can calibrate the prediction models more effectively in the cases of critical errors, which highlights the practicality of our ResCAL in real-time traffic forecasting.

As shown in Fig. 2, our ResCAL can accurately estimate the residuals and drastically reduce the autocorrelation of residuals both temporally and spatially. Fig. 6 (b) shows the qualitative results of prediction models with and without our proposed ResCAL on METR-LA. When the speed drops rapidly (*i.e.*, an anomalous event occurs), STGCN and DCRNN cannot adapt to the changes; thus, they show poor prediction performance in the changed regions (orange lines). For the same case, our ResCAL successfully captures what those models tend to overestimate and corrects them accurately (green lines). Consequently, as a model-agnostic add-on module, our proposed ResCAL allows the prediction model to adapt to the fluctuation of data and consistently improves prediction performance regardless of the prediction model.

Residual Correction in Overall Situations. While our residual correction clearly shows its effectiveness in situations where residuals are correlated, we can also examine its performance when the existing models already correctly predict speeds. Here, we examine our method in overall situations for both METR-LA and PEMS-BAY to demonstrate its consistency. Table 4 shows that our ResCAL consistently improves the baselines on METR-LA and PEMS-BAY. This indicates that deep-learning-based models generate the correlated residuals even with their large number of parameters, and performance improvement in a high error region also leads to improvement in overall situations. For STGCN, our ResCAL achieves

Table 4: Experimental results on METR-LA and PEMS-BAY. A model with a star denotes that its results were obtained from the original work. Otherwise, the results are reproduced as detailed in Section 5.

Data	Models	15min			30min			60min		
		MAE	RMSE	MAPE	MAE	RMSE	MAPE	MAE	RMSE	MAPE
METR-LA	ARIMA*	3.99	8.21	9.60%	5.15	10.45	12.70%	6.90	13.23	17.40%
	FC-LSTM*	3.44	6.30	9.60%	3.77	7.23	10.90%	4.37	8.69	13.20%
	DCRNN [17]	3.17	5.53	8.28%	3.53	6.33	9.63%	4.02	7.32	11.40%
	+ Calibration	3.05	5.32	7.81%	3.44	6.20	9.25%	3.98	7.21	11.23%
	STGCN [27]	3.33	5.77	8.92%	3.74	6.65	10.39%	4.32	7.72	12.52%
	+ Calibration	2.98	5.28	7.73%	3.47	6.26	9.46%	4.10	7.36	11.62%
	GWNet [26]	2.88	5.10	7.30%	3.33	6.03	8.93%	3.91	7.01	10.84%
	+ Calibration	2.88	5.09	7.30%	3.33	6.02	8.85%	3.87	6.99	10.66%
	STAWnet [21]	2.87	5.15	7.44%	3.28	6.03	8.94%	3.78	6.97	10.55%
	+ Calibration	2.85	5.08	7.30%	3.27	5.98	8.81%	3.77	6.94	10.56%
PEMS-BAY	ARIMA*	1.62	3.30	3.50%	2.33	4.76	5.40%	3.38	6.50	8.30%
	FC-LSTM*	2.05	4.19	4.80%	2.20	4.55	5.20%	2.37	4.96	5.70%
	DCRNN [17]	1.40	2.80	2.95%	1.79	3.87	4.04%	2.21	4.81	5.22%
	+ Calibration	1.37	2.75	2.87%	1.76	3.77	3.91%	2.16	4.64	5.00%
	STGCN [27]	2.15	3.75	4.57%	2.42	4.40	5.35%	2.76	5.12	6.31%
	+ Calibration	1.46	2.87	3.07%	1.85	3.79	4.16%	2.27	4.61	5.29%
	GWNet [26]	1.37	2.72	2.90%	1.72	3.65	3.82%	2.03	4.35	4.67%
	+ Calibration	1.36	2.72	2.84%	1.71	3.64	3.79%	2.03	4.33	4.68%
	STAWnet [21]	1.37	2.75	2.88%	1.72	3.63	3.83%	2.01	4.25	4.68%
	+ Calibration	1.36	2.72	2.86%	1.71	3.62	3.81%	2.01	4.25	4.64%

average improvements of 0.28 in MAE, 0.41 in RMSE, and 1.01% in MAPE on METR-LA. Even with the most recent model STAWnet, our ResCAL shows improvements for MAE, RMSE, and MAPE in both METR-LA and PEMS-BAY.

Running Time Analysis. The average computation time required for calibrating the outputs of the base models (*e.g.*, Graph-WaveNet) was measured in real-time inference. It was tested on METR-LA and 12 sequences of Graph-WaveNet outputs were calibrated. A PC with an Intel Xeon Silver 4210R 2.40GHz CPU and a Titan RTX GPU was used in our analysis. On average, the calibration was performed within 9.05ms. That is, the running time of ResCAL is fast enough for practical usage. Note that the inference time of our ResCAL does not depend on the base model.

Table 5: Tuning analysis of ResCAL with Graph WaveNet.

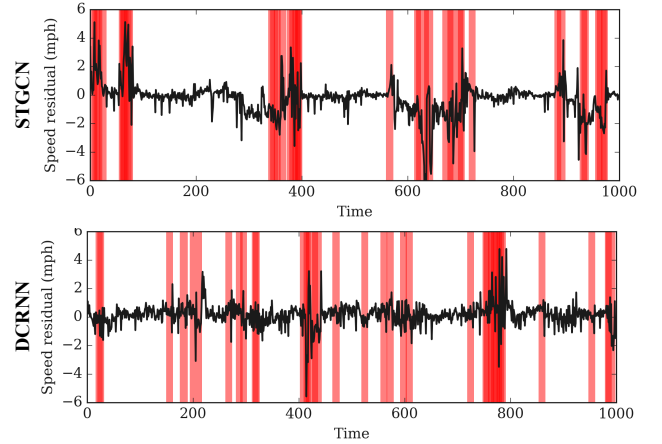
Models	15min			30min			60min		
	MAE	RMSE	MAPE	MAE	RMSE	MAPE	MAE	RMSE	MAPE
STGCN [27]	3.33	5.77	8.92%	3.74	6.65	10.39%	4.32	7.72	12.52%
STGCN-LH	3.43	5.87	9.09%	3.85	6.85	10.84%	4.40	7.95	12.94%
STGCN-LI	3.46	5.84	9.00%	3.90	6.75	10.56%	4.46	7.87	12.77%
STGCN + Ours	2.98	5.28	7.73%	3.47	6.26	9.46%	4.10	7.36	11.62%
Graph-WaveNet [26]	2.88	5.10	7.30%	3.33	6.03	8.93%	3.91	7.01	10.84%
Graph WaveNet-LH	2.90	5.13	7.23%	3.37	6.11	8.72%	4.01	7.22	10.57%
Graph WaveNet-LI	3.31	5.55	8.43%	3.62	6.29	9.66%	4.13	7.17	11.26%
Graph WaveNet + Ours	2.88	5.09	7.30%	3.33	6.02	8.85%	3.87	6.99	10.66%

6.3 Pattern Analysis and Interpretability

Here, we show the qualitative results for the residuals assigned in the same categorical variables to examine the role of the quantization branch of ResCAL. Concretely, we extract the quantized vectors with the dimensions of the number of categorical variables $D = 32$ from the Gumbel-Softmax operation and assign the two residuals in the same pattern if both vectors have identical values for 32 categorical variables. Fig. 7 shows the prediction results of STGCN on METR-LA for the two different input sequences, each from the train dataset and test dataset. The quantized vectors for each pair in Fig. 7 (a), (b), and (c) belong to the same pattern. Notable implication comes from the fact that the residuals assigned to the same category show a similar pattern of the sequences. The results for the train dataset (top) and test dataset (bottom) share a similar ground truth with a similar strategy of calibration. That is, our ResCAL can provide the *interpretable evidences* for calibration. This is crucial for real-time traffic forecasting since the calibration of residuals is mostly needed in the case of unintended failures, and case studies are essential for maintenance of the system.

6.4 Tuning Analysis

In the tuning analysis, we show that the performance gain of ResCAL is mostly based on the consideration of residuals rather than on external factors (e.g., introducing additional parameters). As an add-on module, our ResCAL introduces additional parameters compared to solely using a baseline. In addition, ResCAL uses the residuals from previous predictions, thus observing a wide range of input sequences. For scrutiny, we conducted an experiment to check whether the performance gains can be obtained by simply increasing the model complexity or increasing the input length without using ResCAL. We introduced two variations of the baselines: one with larger parameters (LH) and one with longer input sequences (LI). Concretely, we extend the channels of the convolutional layers to increase the number of parameters as much as our ResCAL ($\sim 170k$) for LH models and provide $2\times$ longer input sequences for the LI models. Table 5 shows the results of the two variations and the original with our ResCAL on METR-LA. Interestingly, even with the larger parameters and wide ranges of usable data, the baselines cannot reproduce the results of our ResCAL. In Graph WaveNet-LH, introducing the larger parameters seems to improve the performance in terms of MAPE. However, the performance of MAE and RMSE significantly decreased, even compared to the original Graph WaveNet. In contrast, the model with our ResCAL shows a stable performance improvement in all cases.

**Figure 8: The residual patterns of the baseline models on METR-LA. The regions of 5% minor patterns are highlighted in red.**

6.5 Sanity Check on Clustering

To validate the reliability of our quantization branch, we performed a sanity check by assessing the patterns with lower occurrences. Fig. 8 highlights 5% of the time steps assigned to the least frequent patterns. From this, we can observe that abnormal residuals mainly occur in the selected regions. This demonstrates that our quantization branch can capture minor patterns faithfully without being biased toward dominant events.

7 CONCLUSION

In this work, we introduce a real-time setting in traffic forecasting and show that the residuals occurring from deep-learning-based models are highly correlated both spatially and temporally. To fully consider the autocorrelation of the residuals, we present a model-agnostic add-on module named ResCAL, which calibrates the predictions by estimating the residuals. Without having to fix the original architectures, which may entail high computational cost, our ResCAL module can effectively capture spatial-temporal dependencies of the residuals. On METR-LA and PEMS-BAY, our ResCAL consistently shows performance improvements for the existing forecasting models in event situations. Furthermore, we demonstrate the high practicality of our ResCAL in real-time traffic forecasting by providing the interpretability for calibration and effectively calibrating the predictions with significant errors. While we focus on traffic datasets, our proposed approach can be freely adopted to various tasks with autocorrelated residuals. We hope that our findings will shed light on future research for other forecasting problems as well as traffic forecasting.

ACKNOWLEDGMENTS

This work was supported by the Institute of Information & communications Technology Planning & Evaluation (IITP) grant funded by the Korean government (MSIT) (No. 2019-0-00075, Artificial Intelligence Graduate School Program (KAIST)), and the National Research Foundation of Korea (NRF) grant funded by the Korean government (MSIT) (No. NRF-2022R1A2B5B02001913). This work was also partially supported by NAVER Corp.

REFERENCES

- [1] James Atwood and Don Towsley. 2016. Diffusion-Convolutional Neural Networks. In *Proc. the Advances in Neural Information Processing Systems (NeurIPS)*.
- [2] George EP Box, Gwilym M Jenkins, and Gregory C Reinsel. 1976. Time series analysis prediction and control.
- [3] Tianqi Chen, Tong He, Michael Benesty, Vadim Khotilovich, Yuan Tang, Hyunsu Cho, et al. 2015. Xgboost: extreme gradient boosting. *R package version 0.4-2* 1, 4 (2015), 1–4.
- [4] Xi Chen, Yan Duan, Rein Houthooft, John Schulman, Ilya Sutskever, and Pieter Abbeel. 2016. InfoGAN: Interpretable Representation Learning by Information Maximizing Generative Adversarial Nets. In *Proc. the Advances in Neural Information Processing Systems (NeurIPS)*.
- [5] Xingyi Cheng, Ruiqing Zhang, Jie Zhou, and Wei Xu. 2018. DeepTransport: Learning Spatial-Temporal Dependency for Traffic Condition Forecasting. In *2018 International Joint Conference on Neural Networks, IJCNN 2018, Rio de Janeiro, Brazil, July 8-13, 2018*.
- [6] Jerome H Friedman. 2001. Greedy function approximation: a gradient boosting machine. *Annals of statistics* (2001), 1189–1232.
- [7] Robert Gray. 1984. Vector quantization. *IEEE Assp Magazine* 1, 2 (1984), 4–29.
- [8] Sepp Hochreiter and Jürgen Schmidhuber. 1997. Long Short-Term Memory. *Neural Comput.* (1997).
- [9] Qian Huang, Horace He, Abhay Singh, Ser-Nam Lim, and Austin R. Benson. 2021. Combining Label Propagation and Simple Models out-performs Graph Neural Networks. In *Proc. the International Conference on Learning Representations (ICLR)*.
- [10] Rob J Hyndman and George Athanasopoulos. 2018. *Forecasting: principles and practice*. OTexts.
- [11] H. V. Jagadish, Johannes Gehrke, Alexandros Labrinidis, Yannis Papakonstantinou, Jignesh M. Patel, Raghu Ramakrishnan, and Cyrus Shahabi. 2014. Big data and its technical challenges. *Commun. ACM* (2014).
- [12] Eric Jang, Shixiang Gu, and Ben Poole. 2017. Categorical Reparameterization with Gumbel-Softmax. In *Proc. the International Conference on Learning Representations (ICLR)*.
- [13] Junteng Jia and Austin R. Benson. 2020. Residual Correlation in Graph Neural Network Regression. In *Proc. the ACM SIGKDD International Conference on Knowledge Discovery and Data Mining (KDD)*.
- [14] Guolin Ke, Qi Meng, Thomas Finley, Taifeng Wang, Wei Chen, Weidong Ma, Qiwei Ye, and Tie-Yan Liu. 2017. LightGBM: A Highly Efficient Gradient Boosting Decision Tree. In *Proc. the Advances in Neural Information Processing Systems (NeurIPS)*.
- [15] Diederik P. Kingma and Jimmy Ba. 2015. Adam: A Method for Stochastic Optimization. In *Proc. the International Conference on Learning Representations (ICLR)*.
- [16] Thomas N. Kipf and Max Welling. 2017. Semi-Supervised Classification with Graph Convolutional Networks. In *Proc. the International Conference on Learning Representations (ICLR)*.
- [17] Yaguang Li, Rose Yu, Cyrus Shahabi, and Yan Liu. 2018. Diffusion Convolutional Recurrent Neural Network: Data-Driven Traffic Forecasting. In *Proc. the International Conference on Learning Representations (ICLR)*.
- [18] Cheonbok Park, Chunggi Lee, Hyojin Bahng, Yunwon Tae, Seungmin Jin, Kihwan Kim, Sungahn Ko, and Jaegul Choo. 2020. ST-GRAT: A Novel Spatio-temporal Graph Attention Networks for Accurately Forecasting Dynamically Changing Road Speed. In *Proc. the ACM Conference on Information and Knowledge Management (CIKM)*.
- [19] David I. Shuman, Sunil K. Narang, Pascal Frossard, Antonio Ortega, and Pierre Vandergheynst. 2013. The Emerging Field of Signal Processing on Graphs: Extending High-Dimensional Data Analysis to Networks and Other Irregular Domains. *IEEE Signal Process. Mag.* 30, 3 (2013), 83–98.
- [20] Ilya Sutskever, Oriol Vinyals, and Quoc V. Le. 2014. Sequence to Sequence Learning with Neural Networks. In *Proc. the Advances in Neural Information Processing Systems (NeurIPS)*, Zoubin Ghahramani, Max Welling, Corinna Cortes, Neil D. Lawrence, and Kilian Q. Weinberger (Eds.).
- [21] Chenyu Tian and Wai Kin (Victor) Chan. 2021. Spatial-temporal attention wavenet: A deep learning framework for traffic prediction considering spatial-temporal dependencies. *IET Intelligent Transport Systems* (2021).
- [22] Aäron van den Oord, Sander Dieleman, Heiga Zen, Karen Simonyan, Oriol Vinyals, Alex Graves, Nal Kalchbrenner, Andrew W. Senior, and Koray Kavukcuoglu. 2016. WaveNet: A Generative Model for Raw Audio. *CoRR* abs/1609.03499 (2016).
- [23] Aäron van den Oord, Oriol Vinyals, and Koray Kavukcuoglu. 2017. Neural Discrete Representation Learning. In *Proc. the Advances in Neural Information Processing Systems (NeurIPS)*.
- [24] Ashish Vaswani, Noam Shazeer, Niki Parmar, Jakob Uszkoreit, Llion Jones, Aidan N. Gomez, Lukasz Kaiser, and Illia Polosukhin. 2017. Attention is All you Need. In *Proc. the Advances in Neural Information Processing Systems (NeurIPS)*.
- [25] Yuankai Wu and Huachun Tan. 2016. Short-term traffic flow forecasting with spatial-temporal correlation in a hybrid deep learning framework. *CoRR* abs/1612.01022 (2016).
- [26] Zonghan Wu, Shirui Pan, Guodong Long, Jing Jiang, and Chengqi Zhang. 2019. Graph WaveNet for Deep Spatial-Temporal Graph Modeling. In *Proc. the International Joint Conference on Artificial Intelligence (IJCAI)*, Sarit Kraus (Ed.).
- [27] Bing Yu, Haoteng Yin, and Zhanxing Zhu. 2018. Spatio-Temporal Graph Convolutional Networks: A Deep Learning Framework for Traffic Forecasting. In *Proc. the International Joint Conference on Artificial Intelligence (IJCAI)*.
- [28] Jiani Zhang, Xingjian Shi, Junyuan Xie, Hao Ma, Irwin King, and Dit-Yan Yeung. 2018. GaAN: Gated Attention Networks for Learning on Large and Spatiotemporal Graphs. In *Proc. the Conference on Uncertainty in Artificial Intelligence (UAI)*.
- [29] Junbo Zhang, Yu Zheng, Dekang Qi, Ruiyuan Li, and Xiuwen Yi. 2016. DNN-based prediction model for spatio-temporal data. In *Proceedings of the 24th ACM SIGSPATIAL International Conference on Advances in Geographic Information Systems, GIS 2016, Burlingame, California, USA, October 31 - November 3, 2016*.
- [30] Chuanpan Zheng, Xiaoliang Fan, Cheng Wang, and Jianzhong Qi. 2020. GMAN: A Graph Multi-Attention Network for Traffic Prediction. *Proc. the AAAI Conference on Artificial Intelligence (AAAI)*.